Effect of perlite nanoclay reinforcements on the mechanical and tribological behaviour of AA7076 metal matrix nanocomposites

G U Raju*
School of Mechanical Engineering, KLE Technological University, Hubballi, India
raju_gu@kletech.ac.in, https://orcid.org/0000-0003-0234-1055

Vinod Kumar V Meti*
Department of Automation & Robotics, KLE Technological University, Hubballi, India
vinod_meti@kletech.ac.in, https://orcid.org/0000-0001-5692-9693

Amitkumar R Nadugeri, I G Siddhalingeshwar
School of Mechanical Engineering, KLE Technological University, Hubballi, India
amitrn1998@gmail.com
igs@kletech.ac.in, https://orcid.org/0000-0002-2361-596X

M. A. Umarfarooq*
Center for Material Science, Karpagam Academy of Higher Education, Coimbatore, Tamil Nadu, India.
Department of Mechanical Engineering Karpagam Academy of Higher Education, Coimbatore, Tamil Nadu, India.
umarfarooq.ma@gmail.com, https://orcid.org/0000-0002-9369-7913

N.R. Banapurmath, Ashok M Sajjan
Centre of Excellence in Material Science, School of Mechanical Engineering, KLE Technological University, Hubballi-580031, India
nr_banapurmath@kletech.ac.in, https://orcid.org/0000-0002-1280-6234
am_sajjan@kletech.ac.in, https://orcid.org/0000-0003-1251-8803

B H Maruthi Prashanth
Department of Mechanical Engineering, AGM Rural College of Engineering and Technology, Varur, Hubballi, Karnataka - 581 207, India
bhmprashant@gmail.com, https://orcid.org/0000-0003-3100-5288

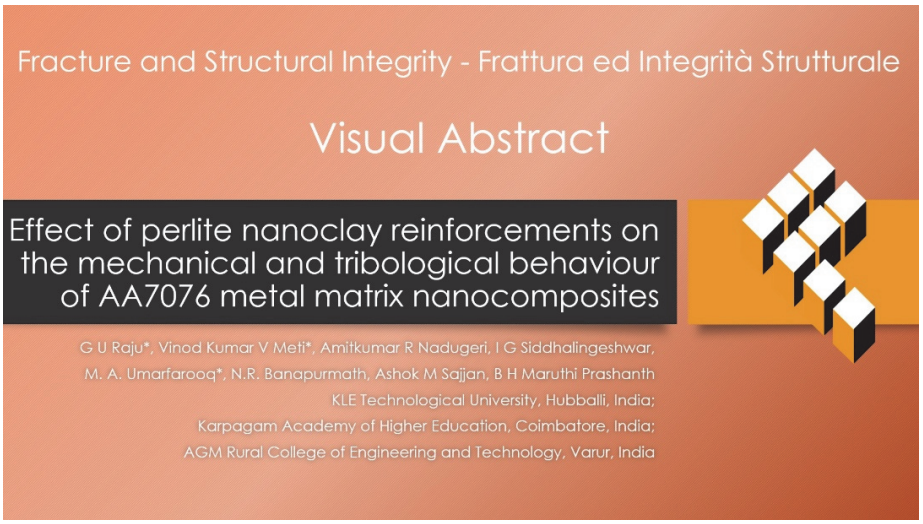

Citation: Raju, G. U., Meti, V. K. V., Nadugeri, A. R., Siddhalingeshwar, I. G., Umarfarooq, M. A., Banapurmath, N. R., Sajjan. A. M., Prashanth, B. H. M., Effect of perlite nanoclay reinforcements on the mechanical and tribological behaviour of AA7076 metal matrix nanocomposites, Fracture and Structural Integrity, 75 (2026) 281-296.

Received: 30.06.2025
Accepted: 04.11.2025
Published: 06.11.2025
Issue: 01.2026

KEYWORDS. AA7076 matrix composites, Perlite nanoclay particle, Stir casting, Mechanical and tribological behaviour.

INTRODUCTION

Aluminium alloys, primarily composed of aluminium (Al) with alloying elements such as copper, manganese, magnesium, silicon, zinc, and tin, are widely used in engineering applications, where strength and lightweight properties are crucial. Around 85% of aluminium is utilised in forged products such as billets, rolled plates, and aluminium foil. While cast aluminium alloys are more affordable due to their lower melting points, they generally have lower tensile strengths compared to forged alloys. Among cast aluminium alloys, Al-Si alloys are particularly popular because of their high silicon content (4-13%), which gives them excellent casting properties. Since the introduction of metal-skinned aircraft, aluminium alloys have been extensively employed in the aerospace industry due to their favourable strength-to-weight ratio [1-3].

Aluminium matrix composites are increasingly used in automotive and aerospace industries due to their superior mechanical properties, lower density, improved corrosion and wear resistance, and lower thermal expansion coefficient. Recent advancements have focused on enhancing these properties through the incorporation of nano-scale reinforcements such as silicon carbide (SiC), boron carbide (B_4C), alumina (Al_2O_3), graphene, and carbon nanotubes (CNTs)

Patel et al. [4-6] conducted a series of studies fabricating AA5052 aluminum matrix composites reinforced with 5 wt.% of either SiC or B4C particles via stir casting. Their results demonstrate that B_4C reinforcement significantly enhances micro-hardness (69.2%) and compressive strength (46.9%) while reducing density (0.68%), making it ideal for lightweight applications. In contrast, SiC reinforcement improves abrasive wear resistance and hardness (39.7%) but increases density (0.8%). Both composites show uniform particle distribution and low porosity, confirming the effectiveness of the stir casting process for developing high-performance composites. Zhu et al. [7] reported enhanced mechanical properties in Al 6082 reinforced with nano-SiC due to uniform dispersion. Wang et al. [8] studied aluminium-based silicon carbide composites and their tribological features, finding that higher SiC content enhanced tensile strength at the cost of reduced ductility. Singh et al. [9] investigated the mechanical and tribological performance of hypereutectic aluminium-silicon alloy composites, reinforced with SiC, observing a 38% increase in tensile strength due to uniform dispersion of reinforcements along the grain boundaries. Patel et al. [10] developed AA5052/B_4C metal matrix composites using stir casting, achieving 71% higher hardness and improved wear resistance compared to pure AA5052, making them suitable for lightweight and wear critical applications. AA7075 reinforced with TiB_2 and ZrO_2 showed an improvement in tensile strength (50%), hardness (20%), and a reduction in wear rate by 70% [11]. Ravikumar et al. [12] reported that reinforcement of AA7075 with hybrid micro and nano Al_2O_3 improved hardness (28%), tensile strength (32%), and up to 40 – 50% reduction in wear rate. Patil et al [13] reported an increase in wear resistance with the addition of MWCNTs (0.5 wt% - 2 wt.%) to AA7076. Raju et al. [14] reported that hybrid Mg-AZ91D composite reinforced with carbon fibers and MWCNTs showed up to 19%

higher hardness, 35% higher tensile strength, and improved wear resistance, owing to uniform reinforcement dispersion and strong interfacial bonding. The wear rate reduction ranged between 4 % to 35 % at different loading conditions (10N, 20N, and 30N). While AA7076 loaded with graphene amine and carbon fiber at 1 wt.% reinforcement achieved an increase in hardness, tensile strength by 50 % and 42% respectively [15]. Studies by Jayaseelan et al. [16] and Nirala et al. [17] further highlighted the potential of graphene and CNT reinforcements in improving tensile strength and wear resistance.

Despite these advances, there remains a need for cost-effective and readily available reinforcements that can be easily integrated into aluminium matrices. Nanoclays, such as perlite nanoclay, offer a promising alternative due to their high aspect ratio, thermal stability, and potential for improving mechanical and tribological properties. While nanoclays have been extensively studied in polymer composites, their application in aluminium MMCs, particularly with AA7076 alloy, has been scarcely explored.

To date, systematic evaluation of perlite nanoclay as a reinforcement in AA7076 alloys has not been reported. This work, therefore, represents the first systematic investigation of perlite nanoclay-reinforced AA7076 composites, highlighting their mechanical and tribological performance and establishing their potential as a cost-effective and sustainable reinforcement material.

EXPERIMENTAL DETAILS

Materials utilised and preparation of MMCs

In this study, perlite nanoclay is employed as a reinforcement. Perlite is a naturally occurring amorphous volcanic aluminosilicate, chemically distinct from pearlite (a steel microstructure), which, when heated to 870 ºC, expands into a lightweight, glassy cellular structure that imparts excellent insulation and low density [18]. The chemical composition is SiO_2 (61.61%), Al_2O_3(8.84%), Fe_2O_3 (16.92%), TiO_2 (1.8%), K_2O(4.11%), MgO(6.02%), and 0.7% others [19]. Tab. 1 depicts the chemical composition of AA7076 alloy, while Tab. 2 provides the properties of perlite nanoclay.

To develop nanocomposites, a base matrix containing perlite nanoclay particles at 1.0 and 1.5 wt.% was used. The AA7076-perlite nanoclay nanocomposite was synthesised using the motorised stir casting technique, as shown in Fig. 1. The AA7076 aluminium was heated to 650°C, and both the aluminium and the perlite nanoclay were preheated in a preheater chamber at a constant temperature of 400°C. The reinforcements were added to the furnace once the preheating was completed. Degasification was performed to remove entrapped gases from the heated liquid melt [20 - 21]. A stirring speed of 400 rpm was maintained throughout the fabrication process to create vortices in the crucible, ensuring uniform dispersion of nanofillers. Finally, the liquid melt was poured into a preheated metallic mould. The Al 7076/perlite nanoclay nanocomposite test samples were prepared in accordance with ASTM standards to evaluate the mechanical and tribological properties.

Si	Fe	Cu	Mn	Mg	Zn	Ti	Al
0.3	0.4	0.5	0.5	1.2	7.0	0.1	90

Table 1: Chemical composition of AA7076 (wt%).

Density (in g/cc)	Melting temperature (°C)	Specific gravity	Average particle size (nm)
0.35 – 0.65	1093	2.2	80 - 100

Table 2: Properties of perlite nanoclay reinforcement particles.

CHARACTERIZATIONS

Hardness Test

The bulk hardness of samples was measured using a Vickers hardness tester as per ASTM E92. Before testing, the surfaces of the base alloy and composites were polished to ensure smoothness. A load of 50 N was applied using a steel ball indenter with a diameter of 5 mm.

Tensile test

The tensile strength of composite specimens was evaluated using a UTM (100 kN). The test was conducted following the ASTM E-8 standard. Fig. 2 displays the dimensions of the tensile test specimen, which were designed following the ASTM E-8 standard.

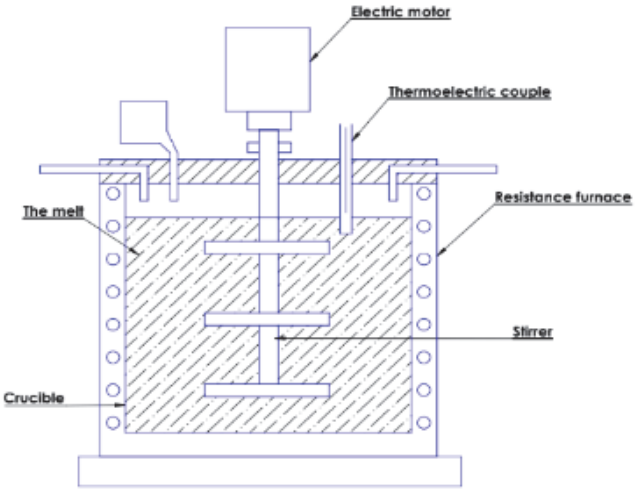

Figure 1: AMC synthesis using the stir casting technique.

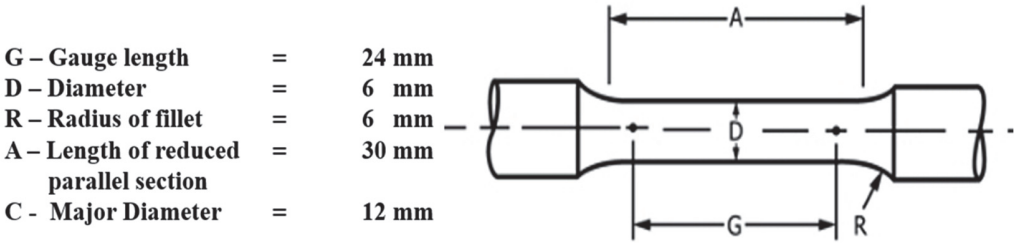

Figure 2: Tensile specimen dimensions.

Dry sliding wear test

The wear resistance of composites was evaluated using a pin-on-disk tribometer under room temperature, as per ASTM G99. Test specimens measuring 6 mm in diameter and 30 mm long were prepared from cast composite bars. The experiments were carried out at different applied loads (10 N, 20 N, and 30 N) with a constant sliding velocity of 1 m/s and a sliding distance of 1200 m for each test.

RESULTS AND DISCUSSIONS

Scanning Electron Microscope (SEM) Analysis

The SEM micrographs and Energy-Dispersive X-ray (EDS) analysis of composite samples provide a clear and informative overview of the material's microstructure. The SEM micrographs in Fig.s 3 (a–d) confirm the presence of perlite nanoclay reinforcement particles within the MMCs. These micrographs illustrate the dispersion of particles within the matrix, providing crucial insights into the structural integrity of the composites. The micrographs demonstrate that the nanoparticles are uniformly distributed along the grain boundaries of the AA7076 matrix. This homogeneous distribution is attributed to the motorised stir-casting process, which effectively disperses the particles throughout the matrix, minimising agglomeration and porosity. This reduction in agglomeration and porosity indicates the effectiveness of the motorised stir-casting technique in achieving uniform dispersion.

EDS Analysis

Figs. 4 (a-d) illustrate the elemental distribution in the AA7076/perlite nanoclay composites obtained from EDX area mapping. Aluminium (Al) (Fig. 4a) appears uniformly across the scanned region, confirming the dominance of the base

alloy matrix. Zinc (Zn) (Fig. 4b), the major alloying element in AA7076, also shows a uniform spread reflecting its even incorporation during casting. Carbon (C) (Fig. 4c) signals the presence of perlite nanoclay reinforcement, since perlite nanoclays contain water and carbon-rich traces from surface functionalization, which remain high after high-temperature processing. Iron (Fe) (Fig. 4d) appears as a localized bright spot, possibly originating from trace Fe_2O_3 content in perlite. The combined mapping confirms the integration of reinforcement particles into the aluminium matrix. Fig. 5 displays peaks corresponding to aluminium (Al) and carbon (C) in the AA7076/perlite nanoclay composites.

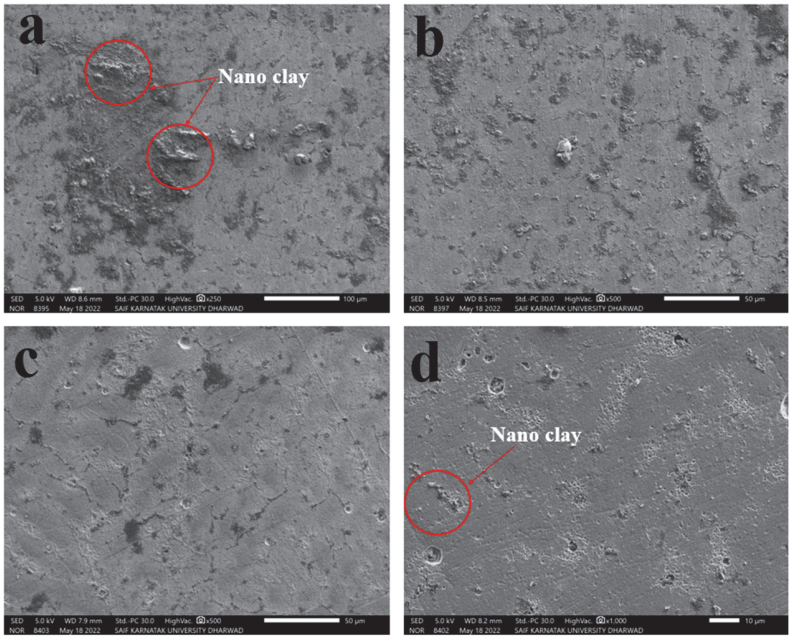

Figure 3 (a-b) SEM micrographs of 1 wt. % nanoclay reinforced composite and (c-d) SEM micrographs of 1.5 wt.% nanoclay reinforced composite.

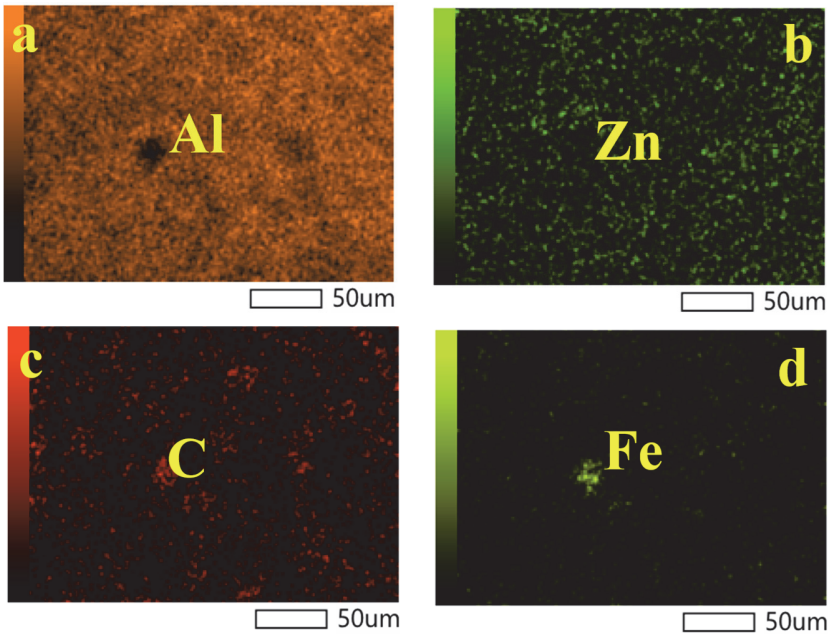

Figure 4 (a-d): EDX spectroscopy for area mapping of Al7076/1% perlite nanoclay composite casting (a) Aluminium (b) Zinc (c) Carbon (d) Iron.

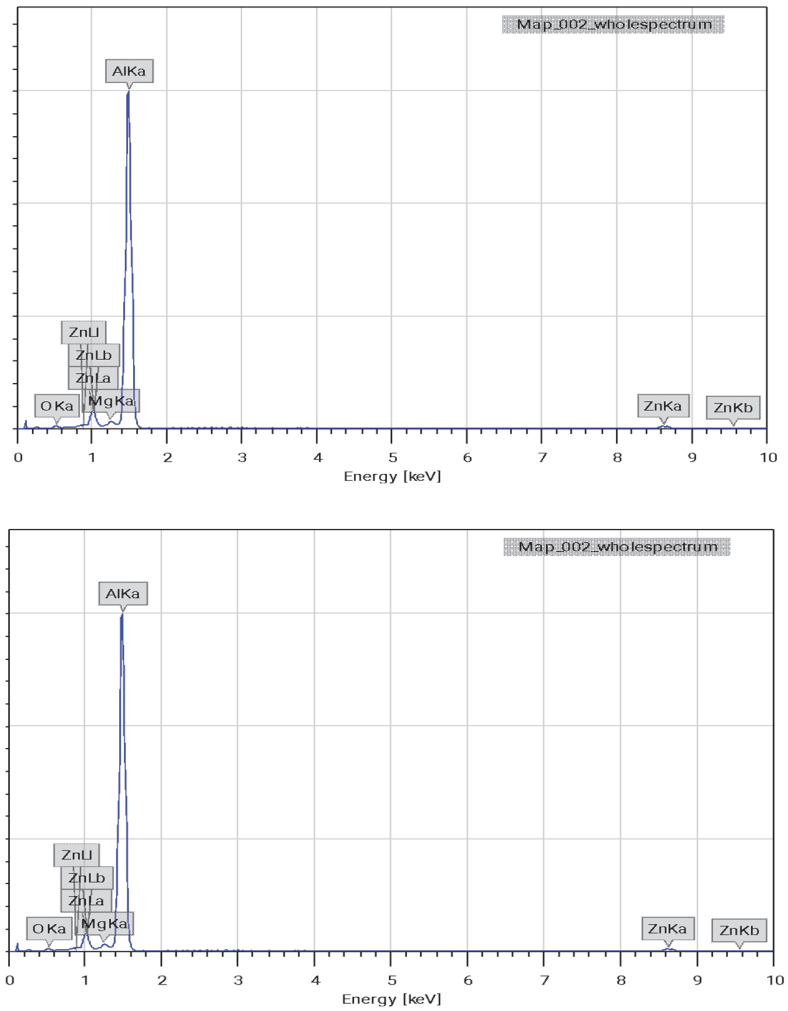

Figure 5: Elemental analysis of the AA7076 composites reinforced with 1 wt. % perlite nanoclay (Top) and 1.5 wt. % perlite nanoclay (Bottom).

MECHANICAL BEHAVIOUR OF NANOCLAY COMPOSITE

Hardness

Fig. 6 illustrates the Vickers hardness of AA7076 composite reinforced with varying weight percentages of perlite nanoclay, providing valuable insights into the impact of these reinforcements on the material's properties. The Vickers hardness of the base material was found to be 82 HV. The addition of perlite nanoclay substantially enhanced the hardness of the AA7076 composite, indicating improved resistance to deformation. Composite loaded with 1 wt.% and 1.5 wt.% perlite nanoclay reinforcement exhibited an enhancement in hardness by 17% and 32% respectively, compared to the aluminium alloy. Increasing the concentration of reinforcement particles positively influences hardness, with the 1.5 wt.% composite exhibiting the highest hardness. The enhanced hardness is attributed to the homogeneous distribution of perlite nanoclay reinforcement around the grain boundaries of AA7076 alloy. Perlite nanoclay particles act as load-absorbing agents, contributing to the ability of the composite to withstand deformation under stress. Similar hardness improvements have been reported in other aluminium-based nanocomposites. Patel et al. [5] observed a 40% increase in hardness in AA5052/SiC composites, while Ravikumar et al. [12] reported a 28% increase in AA7075 reinforced with hybrid Al_2O_3 particles. Harichandran and Selvakumar [11] also demonstrated that the addition of B_4C nanoparticles significantly improved hardness due to their role in restricting dislocation motion.

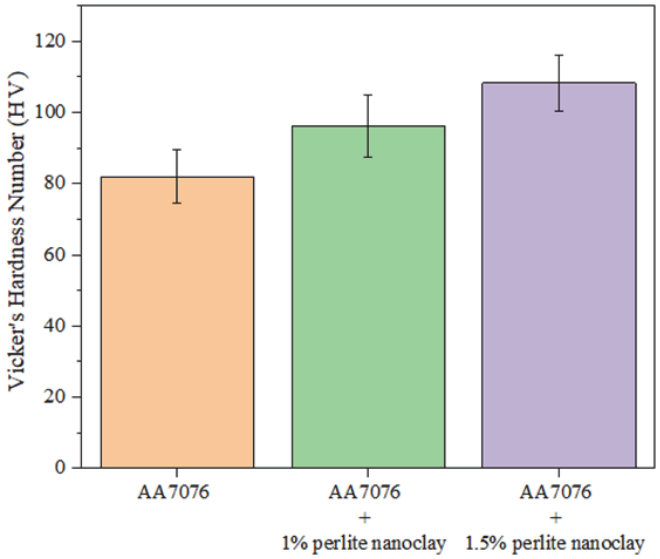

Figure 6: Vickers Hardness of AA7076 and its composites.

TENSILE TEST RESULTS

The stress-strain curves from the tensile tests of AA7076 and its perlite nanoclay-reinforced composites are shown in Fig. 7(a). The tensile strength, modulus, and percentage elongation derived from these curves are shown in Figs. 7(b), 7(c), and 7(d), respectively. The base AA7076 alloy exhibited a tensile strength of 106.15 MPa, a tensile modulus of 1.33 GPa, and a maximum strain of 12.2 %. With the addition of 1 wt.% nanoclay, the tensile strength increased to 126.27 MPa (~ 19% improvement), accompanied by an increase in modulus to 1.77 GPa, while the maximum strain decreased slightly to 11.2%. The 1.5 wt.% nanoclay composite demonstrated the highest tensile strength of 146.39 MPa (~ 38% improvement) and the highest modulus of 2.21 GPa, though the maximum strain dropped further to 8.9%.

These results highlight the beneficial effect of nanoclay on stiffness and load-bearing capacity, but also confirm the typical trade-off between strength and ductility. The improvement in mechanical properties can be attributed to multiple strengthening mechanisms, along with homogeneous dispersion. The nanoscale perlite particles act as a effective barrier to dislocation motion, contributing Orowan strengthening [22], where dislocations bow around the hard inclusions. Additionally, the strong interfacial bonding between the aluminium matrix and nanoclay facilitates efficient load transfer, enhancing tensile strength. The fine distribution of the nanoclay particles also leads to grain boundary pinning, which refines the grain structure and further strengthens the alloy.

Comparable strengthening effects have been reported in earlier studies. Singh et al. [9] observed a 38% increase in tensile strength in Al-Si/SiC composites. The close agreement between these studies and the present work suggests that perlite nanoclay offers a highly efficient strengthening mechanism, achieving similar improvements to higher–loading ceramic reinforcements with the only 1.5 wt.% addition.

The SEM micrographs of the fractured tensile specimens (Figs. 8 (a-d) provide critical insights into the failure mechanisms of the composites. The SEM micrographs (Fig. 8(a-b)) of 1 wt.% loaded exhibit a smoother, flatter fracture surface with dimples, a combination of intergranular cracks, and shallower cleavage facets. These features reflect weaker bonding between matrix and filler particles, providing less for crack propagation. The fracture surface (Fig. 8(c-d)) of 1.5 wt.% demonstrates rougher morphology with dimples, river lines, and particle pull-out. These features indicate strong interfacial bonding between filler particles and the matrix, enabling effective load transfer and resistance to crack propagation. The improved bonding between the matrix and reinforcement particles acts as a barrier to dislocation, further contributing to the increased tensile strength.

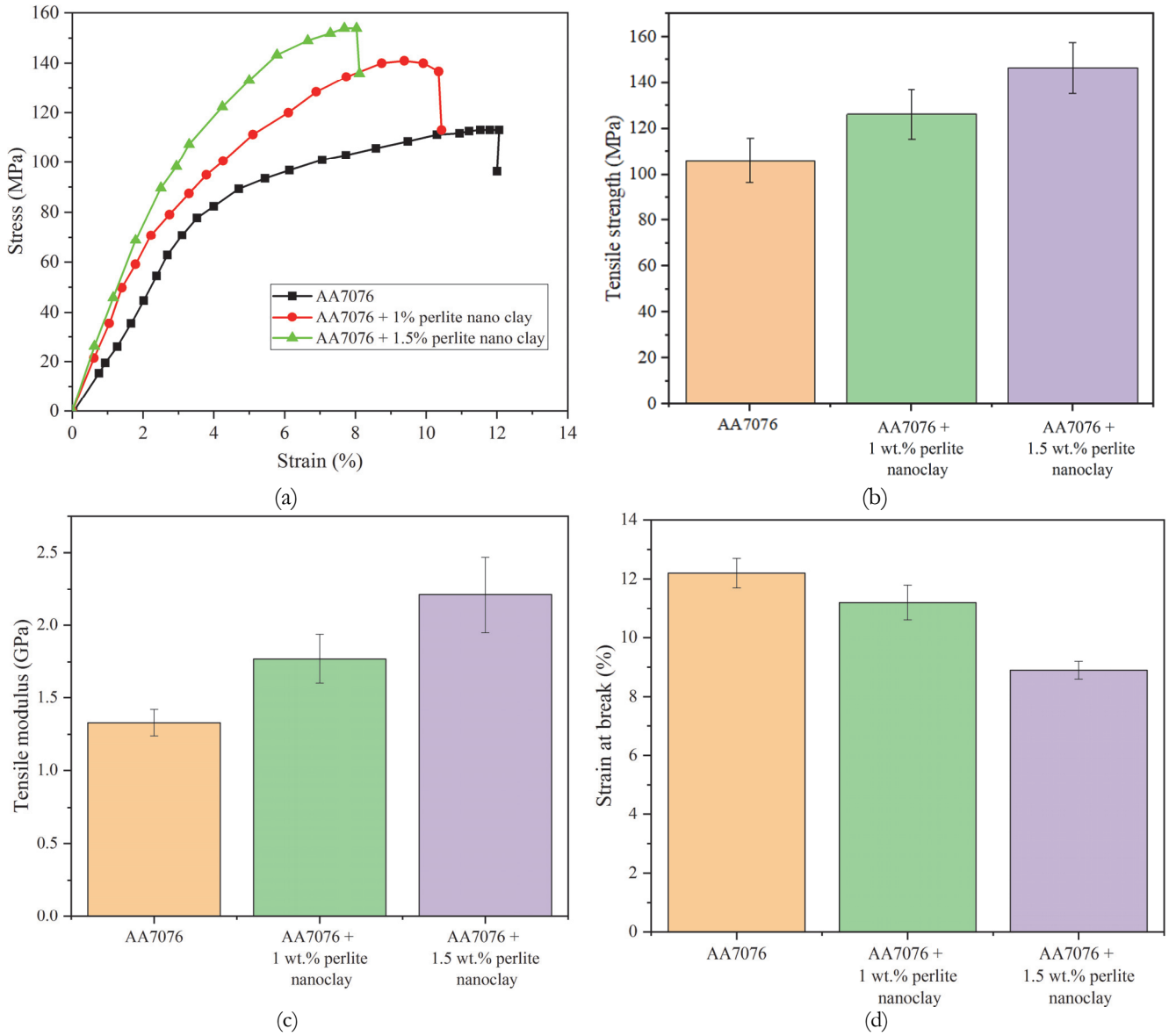

Figure 7: Graphs of (a) Stress-strain curves (b)Tensile strength (c) Tensile modulus (d) Strain at break of AA7076 and their nano-composites reinforced with varying weight percentages of perlite nano-clay

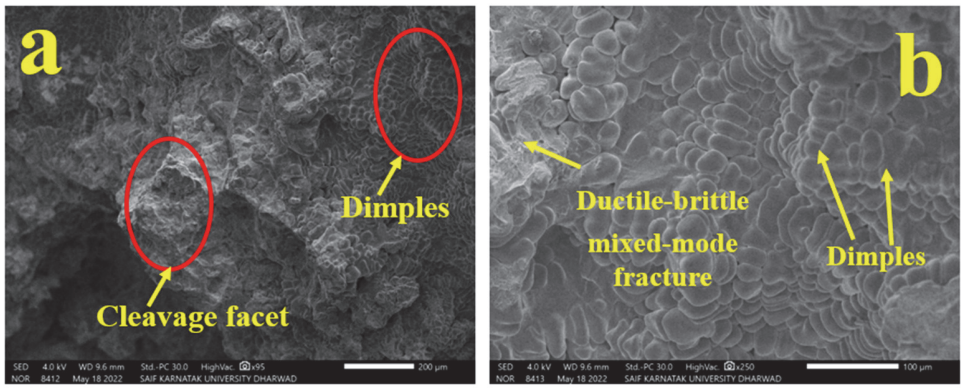

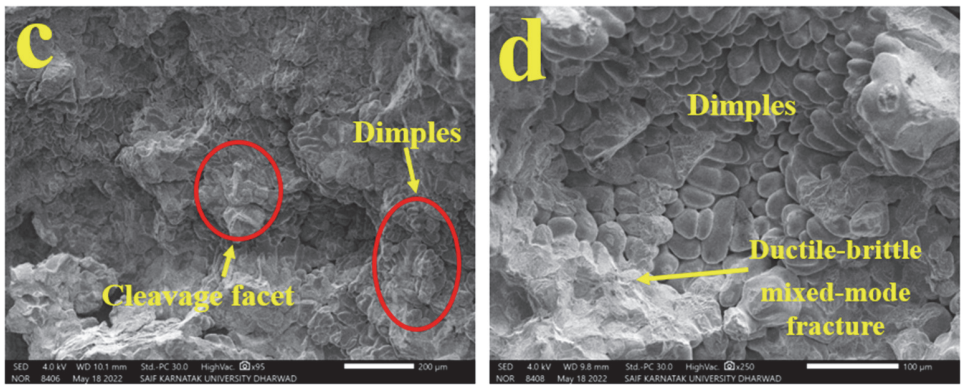

Figure 8: (a-b) SEM micrographs of 1 wt. % nanoclay reinforced composite and (c-d)SEM micrographs of 1.5 wt. % nanoclay reinforced composite,.

TRIBOLOGICAL BEHAVIOUR OF AA7076/PERLITE NANOCLAY COMPOSITE

The wear behaviour of AA7076/perlite nanoclay composites was assessed in terms of wear rate under different applied loads (10,20, and 30N), as shown in Fig. 9. The wear rate of the AA7076 alloy was observed to be 0.0028 mm^3/m, 0.0034 mm^3/m, and 0.0038 mm^3/m at 10 N, 20 N, and 30 N, respectively, confirming that the wear severity increases with load due to higher contact stresses and intensified ploughing at the sliding interface. Incorporation of perlite nanoclay significantly reduced the wear rate across all loading conditions. At 1 wt.% reinforcement, the wear rate decreased to 0.0021 mm^3/m, 0.0027 mm^3/m, and 0.0033 mm^3/m for 10 N, 20 N, and 30 N, respectively. The best performance was achieved with 1.5 wt.% nanoclay, where the wear rate further decreased to 0.0017 mm^3/m, 0.0025 mm^3/m, and 0.003 mm^3/m under the same load conditions. These reductions clearly demonstrate that perlite nanoclay imparts enhanced wear resistance by increasing the hardness, improving load distribution, and providing a lubricating effect at the sliding interface. Similar decreases in wear rate with ceramic reinforcements have been reported for SiC [4] and B_4C [5] based aluminium composites, validating that nanoclay serves as an effective reinforcement for improving the tribological performance of aluminum alloys.

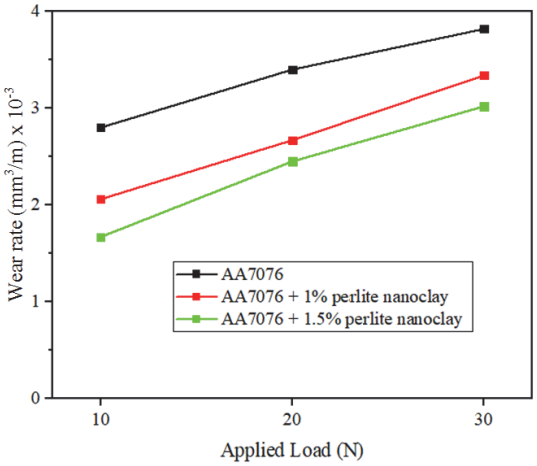

Figure 9: Wear rate of AA7076 composite reinforced with perlite nanoclay.

Analysis of worn surface and wear debris

SEM micrographs of worn surfaces of AA7076-perlite nanoclay composites are shown in Fig. 10 (a-d). The SEM micrographs reveal faint spots on the surface, indicating that material is being removed from the surface in a manner consistent with typical wear patterns. This suggests that the composite material effectively responds to the wear test conditions [16]. The micrographs of 1 wt. % composite (Fig. 10(a-b)) demonstrates deeper grooves, increased surface roughness, and more significant wear debris, indicating relatively higher material removal. However, the 1.5 wt.% composite images (Fig. 10 (c-d)) showed narrower grooves, smoother surfaces, and smaller, less significant wear debris, implying improved wear resistance. This resistance is attributed to the higher hardness of the composite material. Perlite nanoclay

particles impede dislocation movements, enhancing the composite's ability to withstand wear. The uniform dispersion of perlite nanoclay reinforcements in the composite matrix is crucial in enhancing wear resistance. This uniform distribution contributes to the composite's mechanical and tribological properties. The SEM micrographs further show that tracks on the surface are narrow and aligned parallel to the direction of wear. This alignment suggests the presence of a two-body abrasive wear mechanism. In this type of wear, material is removed from the surface due to direct contact and abrasion between the two surfaces in relative motion. Notably, worn debris materials cannot adhere to the surface, and their size is smaller. This is indicative of effective wear resistance, as smaller worn debris particles are less likely to cause additional damage or exacerbate wear.

The SEM micrographs shown in Fig. 11 (a-d) depict the wear debris of AA7076-perlite nanoclay composites, providing important insights into the morphology and composition of debris formed during wear tests. Micrographs of 1 wt. % composites Fig. 11 (a-b) show larger, sharper, and more irregular fragment structures, while 1.5 wt.% composite images Fig. 11 (c-d) depict smaller, flat, and fragmented platelike structures. This variation in morphology demonstrates that increasing filler content influences the debris characteristics, with 1 wt.% exhibiting a more noticeable abrasive wear mechanism. The elemental analysis provided in Fig. 12 reveals the presence of aluminium (Al) and zinc (Zn) as the primary alloying elements along with carbon (C), iron (Fe), and oxygen (O), indicating material transfer, oxidation, and interaction during sliding.

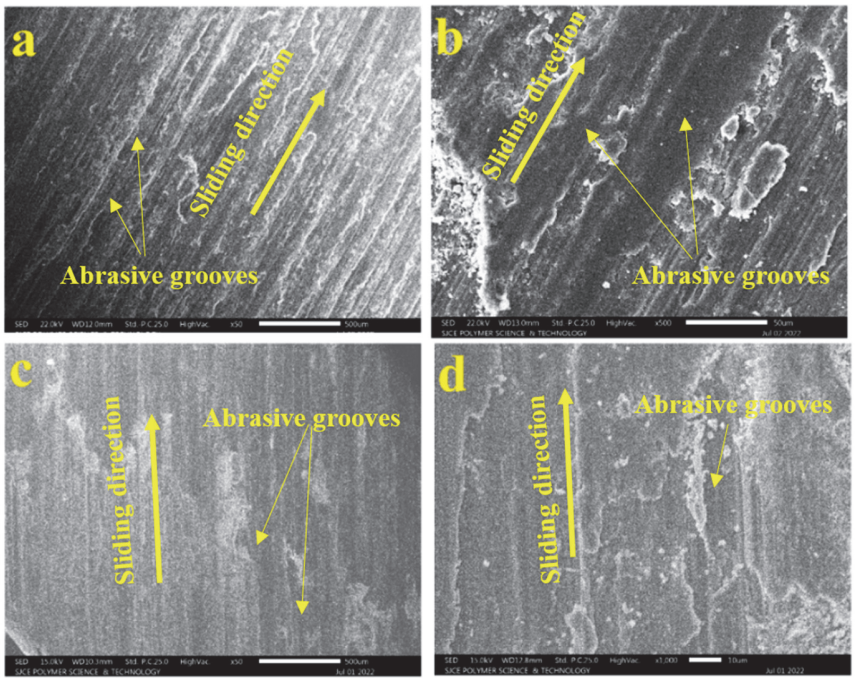

Figure 10: (a-b) SEM micrographs of the worn surfaces of 1 wt. % nanoclay reinforced composite and (c-d) SEM micrographs of the worn surfaces of 1.5 wt. % nanoclay reinforced composite

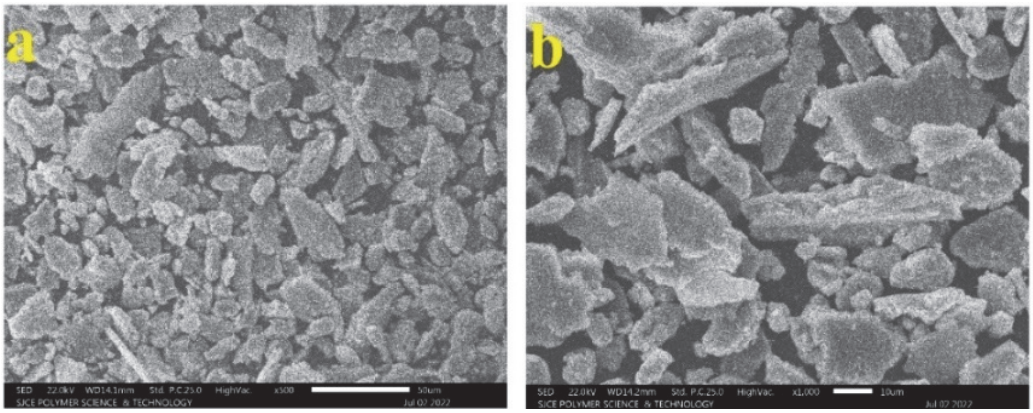

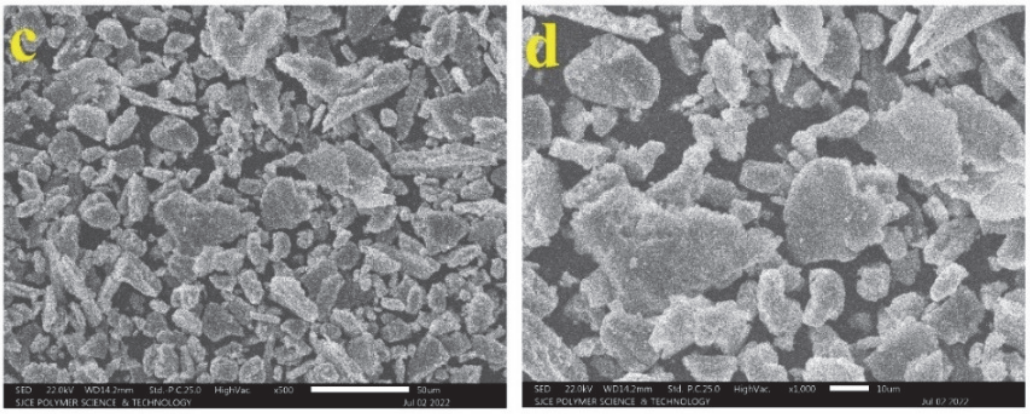

Figure 11: (a-b) SEM micrographs of the wear debris of 1 wt. % nanoclay reinforced composite and (c-d) SEM micrographs of the wear debris of 1.5 wt. % nanoclay reinforced composite.

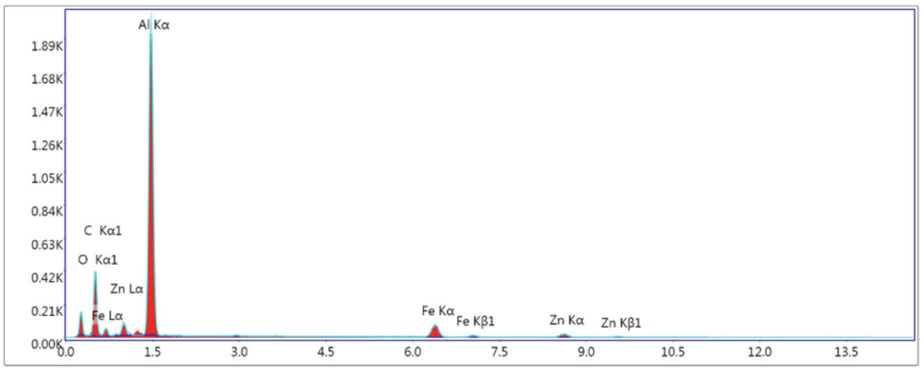

Figure 12: Elemental mapping of wear debris of AA7076 composites reinforced with perlite nanoclay.

SIMULATION STUDIES OF PERLITE NANOCLAY COMPOSITES

A finite element (FE) simulation, carried out using ANSYS Workbench 2023 R1, predicts the mechanical properties of the developed metal nanocomposites, and the results are validated using experimental data.

Development of custom material

In the Engineering Data section of ANSYS Workbench's Material Designer, a custom material was developed by incorporating the properties of AA7076 aluminium alloy and perlite nanoclay. This new material was configured to combine the characteristics of both components for simulation purposes. Representative volume element (RVE) [23 - 24], as shown in Fig. 13(a), was created for each nanocomposite with varying concentrations of nanofillers. The properties of the RVE were taken as input for structural analysis in ANSYS WB.

Discretisation and boundary conditions for tensile test simulation

The CAD model for tensile testing, designed in compliance with ASTM E-8 standards, was developed using CATIA V5. The tensile model was discretised with Solid 92 elements, as illustrated in Fig. 13(b). For the simulation of tensile testing, one end of the specimen was fixed, while an axial load was applied to the opposite end, as depicted in Fig. 13(c). A Static structural analysis was performed on the meshed model to obtain the required results.

A mesh sensitivity (convergence) study was performed on a tensile specimen model to ensure that the FE results are independent of the mesh discretization. Three different element sizes were compared, starting with a coarse mesh of 1mm, followed by a medium mesh of 0.5 mm, and finally a fine mesh of 0.25 mm, using Solid 92 elements. The predicted tensile strength for the 1.5 wt.% composite increased slightly from 154.93 MPa (1 mm mesh) to 156.64 MPa (0.5 mm mesh) and 157.74 MPa (0.25 mm mesh). As shown in Fig. 14, the convergence curve illustrates that the change in predicted tensile strength beyond 0.5 mm element size is negligible (less than 1%), confirming mesh independence. Therefore, the 0.5 mm

mesh was selected for subsequent simulations as it provided an optimal balance between computational efficiency and accuracy.

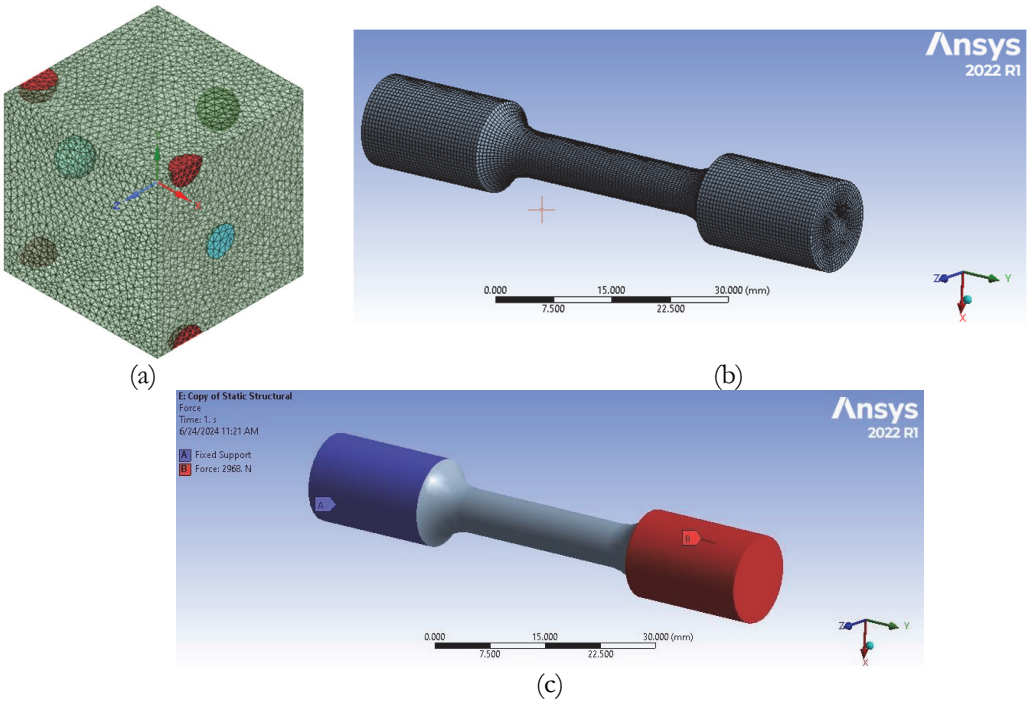

Figure 13: (a) Meshed RVE (b) Meshed tensile test model (c) Boundary conditions applied during tensile test simulation

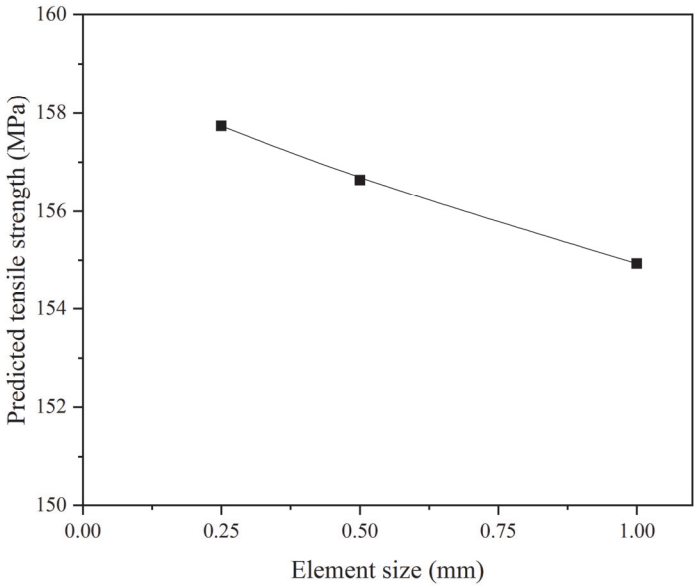

Figure 14: Mesh convergence study.

The tensile strength of the composite samples was determined through simulations conducted in ANSYS Workbench, and the results were compared with experimental data provided in Tab. 3. Fig. 15 illustrates the stress distribution in 1 wt. % nanocomposite specimen. The tensile strength values obtained for the 1 wt. % specimen was 120.16 MPa from the simulation and 126.27 MPa from experimental testing. The variation between the simulated and experimental tensile strength values for all nanocomposites was found to be within a 10% margin.

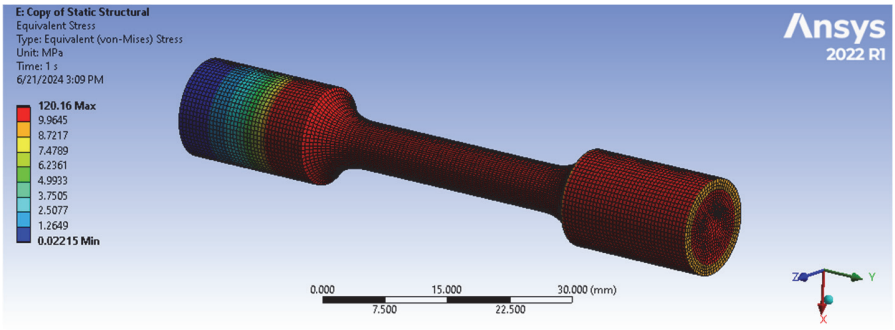

Figure 15: Maximum equivalent stress in S3 tensile specimen.

Nanocomposites	Tensile strength from FE simulation in MPa	Tensile strength from experimental results in MPa	Variation in results (%)
1 wt. % nanoclay	120.16	126.27	4.84
1.5 wt. % nanoclay	157.74	146.39	7.57

Table 3: Simulation results of samples.

Authors	Composite system	Weight fraction of reinforcement	Hardness improvement	Tensile strength improvement	Wear rate reduction	Wear test load range
Present study	AA7076/perlite nanoclay	1 % –1.5%	17% – 38%	19% – 38%	13% – 39%	10 – 30 N
Patil et al. [13]	AA 7076/MWCNTs	0.50 % – 1.50%	–	–	4 % – 35%	10 – 30 N
Patil et al. [15]	AA 7076/ Graphene Amine-Carbon fiber	0.50 % – 1.50%	–	–	(-10%) – – 39%	10 – 30 N
Patel et al. [5]	AA5052/B_4C	5 %	70%	–	–	–
Patel et al. [4,6]	AA5052/SiC	5 %	40%	–	10% – 47%	5 – 15 N
Dhongde et al. [11]	AA7075/ ZrO_2 / 5 % TiB_2 (fixed)	2 – 6% ZrO_2	80 – 85%	5%	–	–
Singh et al. [9]	Al–Si (LM30)/SiC	10 %	17%	38%	–	–
Patel et al. [10]	AA5052/B_4C	5 %	–	–	76% – 84%	5 – 15 N
Nirala et al. [16]	Aluminum/ B_4C/SiC/CNTs	8% B_4C + 2% CNTs 12% B_4C + 2% CNTs 8% SiC + 2% CNTs 12% SiC + 2% CNTs	53% 113% 39% 101%	–	–	–

Table 4: Comparative analysis of mechanical and tribological properties of AA7076/perlite nanoclay with other aluminium matrix.

COMPARATIVE ANALYSIS OF MECHANICAL AND TRIBOLOGICAL PROPERTIES

A critical observation from the comparison of the mechanical and tribological properties of aluminium matrix nanocomposites from the literature with the current work, as presented in Tab. 4, reveals a significant enhancement achieved with a remarkably low weight fraction (1–1.5 wt.%) of perlite nanoclay reinforcement. While many high-performance composites, such as those reinforced with SiC, B_4C, or hybrid systems, require reinforcement loads of 5 wt.% or higher to achieve substantial improvements [5,9,10,16], the present composite demonstrates comparable or higher effectiveness at a fraction of the reinforcement content.

For instance, the maximum improvement in tensile strength (38%) and hardness (38%) for AA7076/perlite nanoclay composite is comparable to the 38% increase in tensile strength reported by Singh et al. [9] using 10 wt.% SiC and the 40%

hardness improvement by Patel et al. [5] using SiC. Notably, the wear rate reduction (up to 39%) is noticeable and outperforms AA7076 composites reinforced with MWCNTs or graphene amine-carbon fibre [13-14].
This demonstrates the exceptional reinforcing efficiency of perlite nanoclay. The ability to achieve property enhancements higher or similar to high-loading or hybrid composites using only 1.5 wt.% reinforcement is a significant advantage.

Limitations

While this study demonstrates significant improvements in the mechanical and tribological properties of AA7076 composites reinforced with perlite nanoclay, this study has certain limitations. First, only two reinforcement levels (1.0 and 1.5 wt.%) were investigated, which restricts the understanding of the full range of composition–property relationships. At higher filler contents, there remains a possibility of particle agglomeration and porosity formation, which could adversely affect performance. Second, the present work is limited to room temperature mechanical and wear testing. High-temperature stability, corrosion resistance, and long-term environmental durability were not evaluated but are critical for aerospace, automotive, and marine applications.

Future works

Building on the present findings, several directions can be pursued in future research. First, exploring higher weight percentages of perlite nanoclay will help to identify the optimum reinforcement level while assessing the risk of agglomeration. Incorporating hybrid reinforcements (combining nanoclay with SiC, CNTs, or graphene) could further enhance mechanical, thermal, and tribological properties through synergetic effects. Second, industrial-scale prototyping and process optimization of stir casting will be essential to evaluate the scalability and economic feasibility of these composites for aerospace and automotive applications. Finally, comprehensive studies on corrosion resistance, high temperature performance, and environmental durability are needed to assess their suitability for real-world operating conditions.

CONCLUSIONS

This study developed and characterized AA7076-based metal matrix nanocomposites reinforced with perlite nanoclay through a motorized stir casting process. The results demonstrate that the 1.5 wt.% nanoclay composite was the optimal composition, exhibiting the highest improvements in hardness (32%), tensile strength (38%), and wear reduction (39%) compared to the unreinforced alloy.
The observed enhancements are attributed to multiple strengthening and wear resistance mechanisms. Uniform dispersion of nanoclay particles across the AA7076 matrix facilitated effective load transfer and restricted dislocation motion. At higher reinforcement loading (1.5 wt.%), the nanoclay further contributed to grain boundary pinning, enabling effective load transfer and wear resistance by reducing ploughing and surface damage.
Numerical simulation studies using ANSYS Workbench further validated the experimental findings. The finite element models predicted tensile strengths within 5 – 8% variation of measured values, demonstrating strong agreement between computational and experimental approaches and confirming the reliability of the developed material model.
Overall, the combination of lightweight AA7076 alloy with perlite nanoclay reinforcement offers a cost-effective, sustainable, and high-performance material. These composites demonstrate strong lightweight potential with superior mechanical and wear properties, suitable for automotive, aerospace, and marine applications.

NOMENCLATURE

σ - tensile stress
ε - strain
HV - hardness value
CoF -coefficient of friction

ACKNOWLEDGEMENT

The author extends heartfelt appreciation to all individuals and institutions whose invaluable support, guidance, and contributions were instrumental in the successful completion of this research.

REFERENCES

[1] Meti, V.K.V., Raju, G.U., Siddhalingeshwar, I.G. and Gaitonde, V.N., (2022). Role of Reinforcement Particle Size and Its Dispersion on Room Temperature Dry Sliding Wear of AA7075/TiB2 Composites. International Journal of Surface Engineering and Interdisciplinary Materials Science (IJSEIMS), 10(1), pp. 1-13. DOI: https://doi.org/10.4018/IJSEIMS.2022010102.

[2] Reddy, G.K., Kumar, B.N., Hareesha, G., Rajesh, A.M. and Doddamani, S., (2023). Investigation of Impact Energy Absorption of AA6061 and Composites: Role of Post-Aging Cooling Methods. Fracture and Structural Integrity, 17(66), pp. 261-272. DOI: https://doi.org/10.3221/IGF-ESIS.66.16.

[3] Ononiwu, N., Ozoegwu, C., Ifeanyi, J., Nwachukwu, V. and Akinlabi, E., (2022). The influence of sustainable reinforcing particulates on the density, hardness and corrosion resistance of AA 6063 matrix composites. Fracture and Structural Integrity, 16(61), pp. 510-518. DOI: https://doi.org/10.3221/IGF-ESIS.61.34.

[4] Patel, M., Sahu, S.K. and Singh, M.K., (2020). Abrasive wear behavior of SiC particulate reinforced AA5052 metal matrix composite. Materials Today: Proceedings, 33, pp. 5586-5591. DOI: https://doi.org/10.1016/j.matpr.2020.03.572.

[5] Patel, M., Sahu, S.K., Singh, M.K. and Dalai, N., (2022). Micro-structural and mechanical characterization of stir cast AA5052/B4C metal matrix composite. Materials Today: Proceedings, 56, pp. 1129-1136. DOI: https://doi.org/10.1016/j.matpr.2021.10.331.

[6] Patel, M., Sahu, S.K. and Singh, M.K., (2020). Fabrication and investigation of mechanical properties of SiC particulate reinforced AA5052 metal matrix composite. Journal of Modern Materials, 7(1), pp. 26-36. DOI: https://doi.org/10.21467/jmm.7.1.26-36.

[7] Zhu, J., Jiang, W., Li, G., Guan, F., Yu, Y. and Fan, Z., (2020). Microstructure and mechanical properties of SiCnp/Al6082 aluminum matrix composites prepared by squeeze casting combined with stir casting. Journal of Materials Processing Technology, 283, p.116699. DOI: https://doi.org/10.1016/j.jmatprotec.2020.116699

[8] Wang, W., Du, A., Fan, Y., Zhao, X., Wang, X., Ma, R., and Li, Q. (2018). Microstructure and tribological properties of SiC matrix composites infiltrated with an aluminum alloy. Tribology International, 120, pp. 369-375. DOI: https://doi.org/10.1016/j.triboint.2018.01.001

[9] Singh, R.K. and Telang, A., (2020). Microstructure, mechanical properties and two-body abrasive wear behaviour of hypereutectic Al—Si—SiC composite. Transactions of Nonferrous Metals Society of China, 30(1), pp. 65-75. DOI: https://doi.org/10.1016/S1003-6326(19)65180-0

[10] Patel, M., Sahu, S.K., Singh, M.K. and Sahu, D.P., (2022). Investigation of tribological properties of stir cast AA5052/B4C MMC under different loads. J. Tribol, 34, pp. 69-86.

[11] Khare, M., Gupta, R.K. and Bhardwaj, B., (2020). Investigation on the Effect of Al_2O_3 and B_4C Ceramic Particles on Mechanical Properties of AA7075 Metal Matrix Composites. SAE international journal of materials and manufacturing, 13(3), pp. 271-296. DOI: https://doi.org/10.4271/05-13-03-0022.

[12] Ravikumar, M., Reddappa, H.N., Suresh, R., Babu, E.R. and Nagaraja, C.R., (2021). Study on Micro-nano sized Al2O3 particles on mechanical, wear and fracture behavior of Al7075 metal matrix composites. Fracture and Structural Integrity, 15(58), pp. 166-178. DOI: https://doi.org/10.3221/IGF-ESIS.58.12.

[13] Patil, A., Banapurmath, N., Hunashyal, A. and Meti, V.K.V. (2022). Wear behavioural studies of MWCNT reinforced AA7076 based nanocomposites. In AIP Conference Proceedings, 2421(1), p. 040003). AIP Publishing LLC. DOI: https://doi.org/10.1063/5.0076782

[14] Raju, G.U., Meti, V.K.V., Banapurmath, N.R., Yunus Khan, T.M., Siddhalingeshwar, I.G., Vaikunte, V., Vadlamudi, C., Krishnappa, S., Sajjan, A.M. and Patil, A. (2022). Effect of multi-walled carbon nanotubes and carbon fiber reinforcements on the mechanical and tribological behavior of hybrid Mg-AZ91D nanocomposites. Materials, 15(17), p.6181. DOI: https://doi.org/10.3390/ma15176181

[15] Patil, A., Banapurmath, N., Hunashyal, A.M., Meti, V. and Mahale, R., (2022). Development and performance analysis of novel cast AA7076-graphene amine-carbon fiber hybrid nanocomposites for structural applications. Biointerface Research in Applied Chemistry, 12(2), pp. 1480-1489. DOI: https://doi.org/10.33263/BRIAC122.14801489.

[16] Jayaseelan, J., Pazhani, A., Michael, A.X., Paulchamy, J., Batako, A. and Hosamane Guruswamy, P.K., (2022). Characterization Studies on graphene-aluminium nano composites for aerospace launch vehicle external fuel tank structural application. Materials, 15(17), p.5907. DOI: https://doi.org/10.3390/ma15175907.

[17] Nirala, A., Soren, S., Kumar, N., Khan, M.A., Islam, S. and Khan, N.A., (2023). Micro-mechanical and tribological behavior of Al/SiC/B4C/CNT hybrid nanocomposite. Scientific Reports, 13(1), p.13147. DOI: https://doi.org/10.1038/s41598-023-39713-2.

[18] Maxineasa, S.G., Isopescu, D.N., Lupu, M.L., Baciu, I.R., Pruna, L. and Somacescu, C., (2022). The use of perlite in civil engineering applications. In IOP conference series: materials science and engineering, 1242(1), p. 012022. IOP Publishing. DOI: https://doi.org/10.1088/1757-899X/1242/1/012022.

[19] Balbuena, J., Sánchez, M., Sánchez, L. and Cruz-Yusta, M., (2024). Lightweight mortar incorporating expanded perlite, vermiculite, and aerogel: a study on the thermal behavior. Materials, 17(3), p.711. DOI: https://doi.org/10.3390/ma17030711.

[20] Suresh, S., Harinath Gowd, G. and Deva Kumar, M.L.S., (2018). Wear behaviour of Al 7075/SiC/Mg metal matrix nano composite by liquid state process. Advanced Composites and Hybrid Materials, 1(4), pp. 819-825. DOI: https://doi.org/10.1007/s42114-018-0054-1

[21] Surappa, M.K., (2003). Aluminium matrix composites: Challenges and opportunities. Sadhana, 28(1), pp. 319-334. DOI: https://doi.org/10.1007/BF02717141.

[22] Liu, H.L., Huang, C.Z., Wang, J. and Sun, J., (2004). Microstructure and mechanical properties of two kinds of Al2O3/SiC nanocomposites. In Materials Science Forum, 471, pp. 243-247. Trans Tech Publications Ltd. DOI: https://doi.org/10.4028/www.scientific.net/MSF.471-472.243.

[23] Nimbagal, V., Banapurmath, N.R., Umarfarooq, M.A., Revankar, S., Sajjan, A.M., Soudagar, M.E.M., Shahapurkar, K., Alamir, M.A., Alarifi, I.M. and Elfasakhany, A., (2023). Mechanical and fracture properties of carbon nano fibers/short carbon fiber epoxy composites. Polymer Composites, 44(7), pp. 3977-3989. DOI: https://doi.org/10.1002/pc.27371.

[24] Dileep, K., Srinath, A., Banapurmath, N., Umarfarooq, M., & Sajjan, A. (2023). Mechanical and Fracture Characterization of Epoxy/PLA/Graphene/SiO2 Composites . Fracture and Structural Integrity, 17(64), pp. 229–239. DOI: https://doi.org/10.3221/IGF-ESIS.64.15.